Investigating the ADP-ribosyltransferase Activity of Sirtuins with NAD Analogues and ^{32}P-NAD[†]

Jintang Du, Hong Jiang, and Hening Lin*

Department of Chemistry and Chemical Biology, Cornell University, Ithaca, New York 14853

Received November 12, 2008; Revised Manuscript Received January 27, 2009

ABSTRACT: Protein ADP-ribosyltransferases catalyze the transfer of adenosine diphosphate ribose (ADP-ribose) from nicotinamide adenine dinucleotide (NAD) onto specific target proteins. Sirtuins, a class of enzymes with NAD-dependent deacetylase activity, have been reported to possess ADP-ribosyltransferase activity, too. Here we used NAD analogues and ^{32}P-NAD to study the ADP-ribosyltransferase activity of several different sirtuins, including yeast Sir2, human SirT1, mouse SirT4, and mouse SirT6. The results showed that an alkyne-tagged NAD is the substrate for deacetylation reactions but cannot detect the ADP-ribosylation activity. Furthermore, comparing with a bacterial ADP-ribosyltransferase diphtheria toxin, the observed rate constant of sirtuin-dependent ADP-ribosylation is >5000-fold lower. Compared with the k_{cat}/K_m values of the deacetylation activity of sirtuins, the observed rate constant of sirtuin-dependent ADP-ribosyltion is ~500 times weaker. The weak ADP-ribosylation events can be explained by both enzymatic and nonenzymatic reaction mechanisms. Combined with recent reports on several other sirtuins, we propose that the reported ADP-ribosyltransferase activity of sirtuins is likely some inefficient side reactions of the deacetylase activity and may not be physiologically relevant.

Sirtuins are a class of enzymes with nicotinamide adenine dinucleotide (NAD)[1] dependent protein deacetylase activity and ADP-ribosyltransferase activity (Figure 1) (*1, 2*). Sirtuins are evolutionally conserved from bacteria to mammals. There are five sirtuins in yeast, Sir2 and Hst1−4, and seven in humans, SirT1−7. Since the initial discovery of the deacetylase activity of sirtuins (*3*), research interest in sirtuins has exploded, and many important functions of sirtuins have been revealed. These functions include the regulation of transcription, apoptosis, genome stability, metabolism, and life span (*2*). Small molecules that can modulate sirtuin activity have been shown to have potential in treating cancer (*4, 5*), Parkinson's disease (*6*), and obesity and diabetes (*7*−*10*), as well as aging and aging-related diseases (*11*).

The NAD-dependent deacetylation mechanism of sirtuins has been elucidated, thanks to the efforts of several laboratories (*12*−*19*). As shown in Figure 1B, the key feature of the mechanism is the α-1′-*O*-alkylimidate intermediate formed upon the displacement of nicotinamide by the attack of the acetyl oxygen. Intramolecular attack by the 2′-OH followed by hydrolysis gives 2′-*O*-acetyl ADP-ribose, which can isomerize to 3′-*O*-acetyl ADP-ribose nonenzymatically. Several crystal structures of sirtuins, including Sir2 from *Archaeoglobus fulgidus* (*20*−*22*), yeast Hst2 (*23*), human SirT2 (*24*), SirT5 (*25*), and *Escherichia coli* CobB (*26*), have been reported. The structures with both NAD and acetyl peptide substrate bound are consistent with the proposed mechanism (Figure 1) (*27*−*29*), and a recent structure further captures the proposed intermediate using a thioacetyl peptide (*30*).

Interestingly, several reports suggested that some sirtuins are protein ADP-ribosyltransferases, which are enzymes that transfer a single ADP-ribosyl group from NAD to proteins (*31*−*33*). Before the discovery of the deacetylation activity of Sir2, it was reported that Sir2 could ADP-ribosylate histones and bovine serum albumin (BSA) (*34*). In 2005, it was reported that mouse SirT6 could self-ADP-ribosylate, and no deacetylation activity could be detected (*35*). In 2006, it was reported that mouse SirT4 could ADP-ribosylate glutamate dehydrogenase (GDH) (*36*), which was shown earlier to be ADP-ribosylated by an unidentified mitochondrial enzyme (*37*). Well-known protein ADP-ribosyltransferases include several bacterial toxins, such as diphtheria toxin (DT), which modifies eukaryotic translation elongation factor 2 (eEF-2) (*38*), and cholera toxin, which modifies Gα (*39*−*41*). Known eukaryotic ADP-ribosyltransferases (termed ARTs) are glycosylphosphatidylinositol-anchored ecto-enzymes that modify membrane or secreted proteins on arginine and cysteine residues (*31, 32*). In addition, most eukaryotic cells have poly(ADP-ribose) polymerases (PARPs) that catalyze the transfer of multiple ADP-ribose units to proteins, typically on glutamate residues (*33, 42, 43*). It has been known for about a decade that intracellular proteins can also be mono(ADP-ribosyl)ated. However, the enzymes responsible have been elusive (*31, 32*). The reported ADP-ribosyltransferase activity of sirtuins has led to the hypothesis

[†] This work is supported in part by the Camille and Henry Dreyfus Foundation New Faculty Award (H.L.).

* To whom correspondence should be addressed. Phone: 607-255-4650. Fax: 607-255-1903. E-mail: hl379@cornell.edu.

[1] Abbreviations: ADP-ribose, adenosine diphosphate ribose; CD38, cluster of differentiation 38; DT, diphtheria toxin; eEF-2, eukaryotic translation elongation factor 2; GDH, glutamate dehydrogenase; MBP, maltose-binding protein; NAD, nicotinamide adenine dinucleotide, oxidized form; PCR, polymerase chain reaction; Sir2, silencing information regulator-2.

10.1021/bi802093g CCC: $40.75
Published on Web 02/16/2009

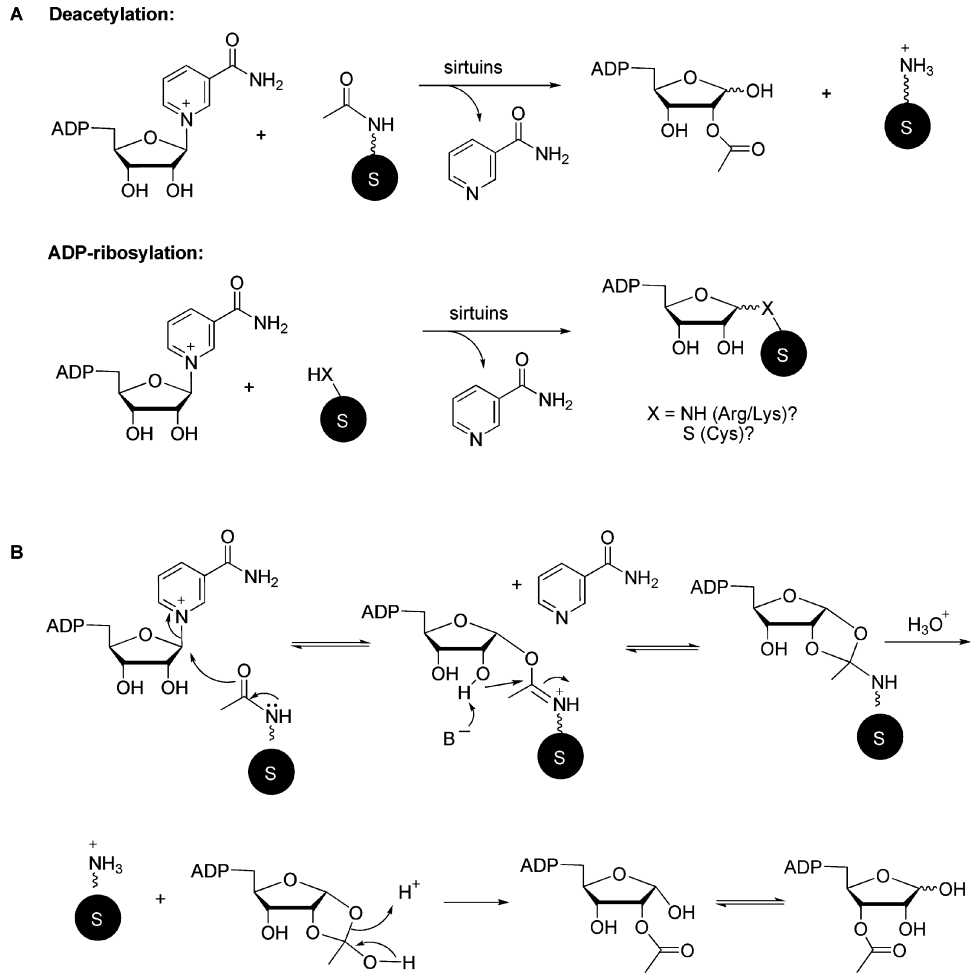

FIGURE 1: (A) Sirtuin-catalyzed deacetylation and ADP-ribosylation reactions. (B) Mechanism of sirtuin-catalyzed NAD-dependent deacetylation.

that sirtuins could be the unknown intracellular protein ADP-ribosyltransferases (*31, 32*).

The reported ADP-ribosyltransferase activity of sirtuins raised interesting questions about the mechanism and the physiological relevance. We are interested in finding out the mechanism for sirtuin-dependent ADP-ribosylation reaction and whether other proteins can also be regulated by sirtuin-catalyzed ADP-ribosylation. To do this, we thought that a general method to label, isolate, and identify ADP-ribosylation substrates of sirtuins would be useful, since this would allow the identification of proteins regulated by ADP-ribosylation and the modified amino acid residues. Here we describe our effort to develop such a method. Surprisingly, in the process of developing such a method, we found that the reported ADP-ribosylation activity of sirtuins is very weak, raising questions about its physiological relevance.

EXPERIMENTAL PROCEDURES

Reagents and Instrumentation. Reagents were obtained from Aldrich or Acros in the highest purity available and used as supplied. ^{1}H NMR was performed on INOVA 500/600 spectrometers, ^{13}C NMR was performed on an INOVA 500 spectrometer, and 2D NMR was performed on INOVA 600 spectrometers. NMR data were analyzed by MestReNova (version 5.2.5). LCMS was carried out on a Shimadzu LCMS-QP8000α with a Sprite Targa C18 column (40 × 2.1 mm, 5 μm; Higgins Analytical, Inc., Mountain View, CA) monitoring at 215 and 260 nm. Solvents were water with 0.1% formic acid and acetonitrile with 0.1% formic acid. Preparative HPLC experiments were accomplished on a Beckman Coulter System Gold 125P solvent module and 168 detector with a Targa C18 column (250 × 20 mm, 10 μm; Higgins Analytical, Inc., Mountain View, CA) monitoring at 215 and 260 nm. Mobile phases used were 0.1% trifluoroacetic acid (TFA) aqueous solution (solvent A) and acetonitrile with 0.1% TFA (solvent B). Compounds were eluted at a flow rate of 10 mL/min with 0% solvent B for 5 min, followed by a linear gradient from 0% to *X*% (*X* depends on different compounds) of solvent B over 60 min. Syntheses of 6-alkyne AMP, 8-alkyne AMP, and Rh-N_3 have been reported (*44*).

Synthesis of 6-Alkyne NAD. To a solution containing nicotinamide mononucleotide (triethylammonium salt, 13.1 mg, 30 μmol) in dioxane (210 μL), *N*,*N*-dimethylformamide (DMF, 75 μL), and hexamethyl phosphoamide (75 μL) were added diphenyl phosphochloridate (12.5 μL, 60 μmol), tri-*n*-butylamine (17.9 μL, 75 μmol), and benzyltributylammonium chloride (9.4 mg, 30 μmol). The mixture was vigorously stirred at room temperature for 1 h under N_2. Then dry ether (10 mL) was added to the reaction mixture, and some precipitate formed. The precipitate was collected by centrifugation, washed with dry ether (10 mL), and dried *in vacuo*. The residue was dissolved in dioxane (150 μL). 6-Alkyne AMP (triethylammonium salt, 21.9 mg, 45 μmol)

in anhydrous DMF (150 μL) was added to the above activated nicotinamide mononucleotide solution, and anhydrous pyridine (150 μL) was added to the mixture immediately. The reaction mixture was stirred overnight at room temperature. After removal of the solvents *in vacuo*, the residue was dissolved in water (5 mL) and purified by HPLC. HPLC fractions were checked by LCMS, and those that contained the product were lyophilized to give the product as a white solid (6.3 mg, 30% yield). Preparative HPLC condition: t_R = 24 min with a linear gradient of 0−40% solvent B over 60 min. ^{1}H NMR (600 MHz, D_2O): 9.42 (s, 1H), 9.27 (d, 1H, J = 6.0 Hz), 8.93 (d, 1H, J = 8.4 Hz), 8.63 (s, 1H), 8.45 (s, 1H), 8.28 (t, 1H, J = 7.2 Hz), 6.16 (d, 2H, J = 5.4 Hz), 4.76 (1H, overlapping with H_2O peak), 4.59 (m, 1H), 4.55 (t, 1H, J = 5.4 Hz), 4.51 (t, 1H, J = 4.5 Hz), 4.46 (dd, 1H, J = 4.8, 2.4 Hz), 4.44 (br, 2H), 4.40 (m, 1H), 4.38 (m, 1H), 4.26 (m, 2H), 4.21 (m, 1H), 2.78 (s, 1H). ^{13}C NMR (125 MHz, 1:1 D_2O:CD_3OD): 166.19, 150.74, 148.69, 147.31, 147.18, 144.12, 143.20, 141.14, 135.24, 129.80, 120.00, 101.48, 89.15, 88.79, 85.63, 79.10, 77.86, 76.22, 75.23, 72.47, 71.78, 66.42, 32.40. LCMS (ESI) calcd for $C_{24}H_{30}N_7O_{14}P_2$ [M^+] 702.1, obsd 701.6. The ^{1}H NMR and ^{13}C NMR assignments are shown in the Supporting Information.

Synthesis of 8-Alkyne NAD. The procedure was the same as that used to make 6-alkyne NAD except that 8-alkyne AMP (triethylammonium salt) was used. 8-Alkyne NAD (6.3 mg) was obtained in 30% yield. Preparative HPLC condition: t_R = 26 min with a linear gradient of 0−40% solvent B over 60 min. ^{1}H NMR (500 MHz, D_2O): 9.44 (s, 1H), 9.28 (d, 1H, J = 6.5 Hz), 8.96 (d, 1H, J = 8.0 Hz), 8.31 (dd, 1H, J = 8.0, 6.0 Hz), 8.28 (s, 1H), 6.18 (d, 1H, J = 5.5 Hz), 6.01 (d, 1H, J = 7.0 Hz), 4.82 (1H, overlapping with H_2O peak), 4.60 (m, 1H), 4.57 (t, 1H, J = 5.3 Hz), 4.51 (dd, 1H, J = 6.0, 3.0 Hz), 4.48 (dd, 1H, J = 5.0, 2.5 Hz), 4.40 (m, 1H), 4.35 (m, 1H), 4.27 (m, 5H), 2.62 (t, 1H, J = 2.5 Hz). ^{13}C NMR (125 MHz, D_2O): 165.78, 153.02, 149.21, 146.60, 146.22, 142.74, 142.32, 140.13, 134.10, 128.90, 116.58, 100.18, 87.36, 87.30, 87.20, 84.44, 84.38, 80.49, 77.78, 72.24, 71.19, 70.96, 70.09, 65.59, 65.10, 32.13. LCMS (ESI) calcd for $C_{24}H_{31}N_8O_{14}P_2$ [M^+] 717.1, obsd 716.3.

Acetylated Histone H3K9Ac 4−15 Peptide Synthesis. Acetylated 12-mer histone H3 peptide (H3K9Ac), corresponding to residues 4 to 15 of the histone H3 N-terminal tail, H_2N-KQTAR(AcK)STGGKA-COOH, was synthesized on Fmoc-Wang resin using the standard Fmoc/*t*Bu chemistry *O*-benzotriazolyl-*N*,*N*,*N*′,*N*′-tetramethyluronium hexafluorophosphate/1-hydroxybenzotriazole (HBTU/HOBt) protocol (*45*). Acetyl lysine was incorporated using Fmoc-Lys(Ac)-OH. The peptides and all protecting groups were cleaved from the resin with TFA containing isopropylsilane (2.5%) and water (2.5%) for 2 h. The crude peptides were purified by reverse-phase HPLC using a Targa C18 column (250 × 20 mm, 10 μm; Higgins Analytical, Inc.) with a linear gradient of 0−50% solvent B. The identity and purity of the peptides were verified by LCMS.

Plasmid Construction. The *Saccharomyces cerevisiae* eEF-2 coding sequence was PCR-amplified by using primers HL009_ScEF-2_5′*Spe*I (5′-AGTCAGACTAGTATGGTTGCTTTCACTGTTGAC-3′) and HL010_ScEF-2_His3′*Xho*I (5′-TCAGCTCGAGTTAATGGTGATGATGGTGGTGATGGTGCAATTTGTCGTAATATTCTTGC-3′). Amplified product was digested with *Spe*I and *Xho*I. The digested PCR product was purified and ligated into the similarly digested expression vector p423Gal1 (ATCC, Manassas, VA). DT F2 fragment (*46*), *SirT1*, *SirT5*, and *Hst2* were cloned using TOPO and Gateway cloning technology (Invitrogen Corp., Carlsbad, CA) into pDEST-F1, and *Sir2*, *SirT2*, *SirT3*(102−399), and *SirT6* were cloned into pDEST-566 for expression.

Expression and Purification of His$_6$-Tagged eEF-2, DT F2 Fragment, Sir2, Hst2, SirT1, SirT2, SirT3(102−399), SirT5, and SirT6. The plasmid *p423Gal1-eEF-2 (pHL007)* was transformed into *S. cerevisiae* strain BY4742 (Open Biosystems, Huntsville, AL). To express the eEF-2 protein, the transformed BY4742 cells were grown in galactose media lacking histidine to OD_{600} of 1.5. Cells were harvested by centrifugation and suspended in 20 mM Tris-HCl buffer (pH 8.0) containing 500 mM NaCl, 10 mM $MgCl_2$, 5 mM imidazole, and protease inhibitors. Cells were lysed using an EmulsiFlex-C3 cell disruptor (Avestin, Inc., Canada), and cell lysate was clarified by centrifugation at 20000 rpm for 30 min and incubated with 1.2 mL of Ni-NTA resin (Qiagen, Valencia, CA) for 1 h at 4 °C. The eEF-2 protein was eluted from resin by 25, 100, 150, and 200 mM imidazole in 20 mM Tris-HCl buffer (pH 8.0) with 500 mM NaCl and 10 mM $MgCl_2$. The eEF-2 protein was further purified by anion exchange on a UNO Q1 column (Bio-Rad Laboratories, Hercules, CA) and gel filtration on a HiLoad 26/60 Superdex 200 prep grade column (GE Healthcare, Piscataway, NJ). The identity of the protein was confirmed by Western blot (detecting His_6 tag) and MALDI-MS analysis of peptides from trypsin digestion.

DT F2 fragment, MBP-Sir2, Hst2, SirT1, MBP-SirT2, MBP-SirT3(102−399), SirT5, and MBP-SirT6 were expressed in *E. coli* BL21 pRARE2 strain. Cells were first cultured in LB media at 37 °C and 200 rpm to OD_{600} ~0.5. The temperature was then changed to 15 °C, and the expression was induced by adding isopropyl β-D-thiogalactoside (IPTG) to 0.1 mM. After incubation at 15 °C for 20 h, cells were harvested by centrifugation (6000 rpm, 10 min) and resuspended in 20 mM Tris-HCl buffer (pH 8.0) with 500 mM NaCl, 10 mM $MgCl_2$, and 5 mM imidazole. Proteins were purified using Ni-NTA resin using the same procedure as used for the purification of eEF-2. MBP-Sir2, Hst2, SirT1, MBP-SirT2, MBP-SirT3(102−399), SirT5, and MBP-SirT6 were further purified by gel filtration. Protein concentrations were determined using the method of Bradford or estimated by comparing Coomassie brilliant blue staining with BSA standards after SDS−PAGE.

Immunoprecipitation of Flag-Tagged SirT4. HeLa cells were grown on ten 100 mm × 20 mm dishes and transfected with *SirT4-pCMV4a* (*36*) using GeneJuice (VWR, West Chester, PA) following the supplier's instruction. After 48 h, cells were collected using a cell scraper and lysed for 30 min at 4 °C in ice-cold lysis buffer (Flag-tagged protein immunoprecipitation kit; Sigma) containing protease cocktail inhibitor (P8340; Sigma). The lysate was clarified by centrifugation (14000 rpm, 15 min) at 4 °C in a microcentrifuge and immunoprecipitated at 4 °C for 4 h following instructions from Sigma. The precipitate was washed once with wash buffer, and then the SirT4 protein was eluted by incubating in elution buffer for 30 min at 4 °C. The presence

of SirT4 protein was confirmed by Western blot using anti-Flag antibody.

Preparation of Yeast Extracts. Yeast extracts were prepared as described elsewhere with modifications (*46*). Wild-type BY4742 and *dph1*-deletion strain YIL103W (ATCC, Manassas, VA) were grown in 20 mL of YPD to OD_{600} of approximately 1, harvested by centrifugation, and washed with 1 mL of buffer (200 mM Tris-HCl, pH 7.5, 400 mM ammonium sulfate, 10 mM magnesium chloride, 1 mM EDTA, 10% glycerol, 1 mM phenylmethanesulfonyl fluoride, and 7 mM β-mercaptoethanol). The cell pellet was resuspended in 0.4 mL of the above buffer and vortexed four times (1 min each time, with 1 min intervals on ice) in the presence of 0.3 g of acid-washed glass beads (0.45 mm diameter; Sigma). The extracts were centrifuged for 15 min at 10000*g*. The supernatants were collected, and the buffer was exchanged to 25 mM Tris-HCl (pH 8.0) with 50 mM NaCl using a centrifugal filter (Millipore, Billerica, MA). The extracts were stored at −80 °C.

Deacetylation Assay. The deacetylase activity of yeast Sir2, Hst2, human SirT1, SirT2, SirT3, and SirT5 was measured by detecting the deacetylated peptide from a H3K9Ac(4−15) using HPLC. In short, purified sirtuin was incubated with 0.5 or 1 mM H3K9Ac(4−15) in 20 mM Tris-HCl buffer (pH 7.5) containing NAD or 6-alkyne NAD (0−750 μM) and 1 mM dithiothreitol (DTT) in 30 or 150 μL reactions. For MBP-Sir2 and Hst2, it was incubated at 30 °C, and other human sirtuins were incubated at 37 °C. The reactions were stopped with 100 mM HCl and 160 mM acetic acid. The reactions were then analyzed by HPLC with a reverse-phase C18 column (250 × 4.6 mm, 90 A, 10 μm; GraceVydac, Southborough, MA), with a linear gradient of 0−20% solvent B for 10 min (1 mL/min). Product quantification was based on the area of absorption monitored at 215 nm, assuming hydrolysis of the acetyl group does not affect the absorption. The k_{cat} and K_m values were obtained by curve fitting the $V_{initial}$/[E] ∼ [S] plot using KaleidaGraph. The experiments were done in duplicate.

ADP-ribosylation Assay of DT-Catalyzed eEF-2 Modification Using NAD Analogues. Purified yeast eEF-2 and 6- or 8-alkyne NAD (50 μM) were incubated with DT (100 nM) for 30 min at 30 °C in 25 mM Tris-HCl (pH 8.0) and 50 mM NaCl. Then Rh-N_3 (in DMF) was added to each reaction to a final concentration of 100 μM, followed by the addition of tris[(1-benzyl-1*H*-1,2,3-triazol-4-yl)methyl]amine (in DMF, final concentration 600 μM), $CuSO_4$ (in water, final concentration 1 mM), and TCEP (in water, final concentration 1 mM) (*47, 48*). After the click chemistry was allowed to proceed at room temperature for 30 min, the reaction mixture was resolved by SDS−PAGE. For ADP-ribosylation reaction using yeast extract, the condition was similar except that 100 μM 6- or 8-alkyne NAD and 200 μM Rh-N_3 were used. For measuring the IC_{50} of NAD inhibiting the labeling of eEF-2 with 6-alkyne NAD and 8-alkyne NAD, 0.5 μg of eEF-2 was incubated with DT (100 nM), 50 μM 6- or 8-alkyne NAD, and different concentrations of NAD. Rhodamine fluorescence signal from protein gel was recorded by a Typhoon 9400 variable mode imager (GE Healthcare Life Sciences), with setting of Green (532 nm)/550BP20 PMT450V (normal sensitivity), and analyzed by ImageQuant TL v2005.

Sirtuin-Dependent ADP-Ribosylation Assay Using NAD Analogues. For sirtuin ADP-ribosylation assays, initially we used the same conditions as those used for the DT-catalyzed eEF-2 ADP-ribosylation. Under these conditions, histones, GDH, and sirtuins were weakly labeled, but the labeling was not dependent on sirtuins. By changing the buffer to 50 mM Tris-HCl, pH 8.0, 150 mM NaCl, and 1 mM DTT, the background labeling can be suppressed, but the sirtuin-dependent ADP-ribosylation was still not observed.

ADP-ribosylation Assay Using ^{32}P-NAD. In 30 μL reactions (50 mM Tris-HCl, pH 8.0, 150 mM NaCl, 10 mM DTT), 5 μCi of ^{32}P-NAD (800 Ci/mmol; American Radiolabeled Chemicals, Inc., St. Louis, MO) was added, and the reactions were incubated at 30 °C for 2 h. For DT-catalyzed yeast eEF-2 ADP-ribosylation, 100 nM DT and 2.0 μg of eEF-2 were used. For sirtuin-catalyzed ADP-ribosylation reactions, 3.7 μg of MBP-Sir2, 1.4 μg of SirT1, and 5 μg of calf thymus histones (Roche Applied Science, Indianapolis, IN) were used. After the 2 h incubation, proteins were precipitated by 20% trichloroacetic acid and washed with acetone twice. Precipitated proteins were resuspended in protein loading buffer, heated at 95 °C for 10 min, and then resolved by SDS−PAGE on 16% polyacrylamide gels. Gels were stained with Coomassie blue, dried, and exposed to a phosphorimaging screen (GE Healthcare, Piscataway, NJ). The signal was detected using a STORM860 phosphorimager (GE Healthcare, Piscataway, NJ). Quantification was performed using ImageQuant TL v2005 (GE Healthcare, Piscataway, NJ) with lane-specific background subtraction.

For the labeling reactions using ^{32}P-ADP-ribose, 5 μCi of ^{32}P-NAD was incubated with 10 nM CD38 for 5 min at room temperature. This condition was sufficient to convert all NAD to ADP-ribose based on the HPLC analysis of similar reactions with cold NAD. Then histone was added to initiate the ADP-ribosylation reaction. The labeling was detected similarly as described above.

HPLC Analysis of NAD Hydrolysis. Reactions (60 μL) were carried out in 20 mM Tris-HCl buffer, pH 7.5, with either 200 or 5 μM NAD. Reactions were initiated by the addition of CD38 or sirtuins. Sirtuins analyzed included MBP-Sir2 (20 μg), SirT1 (10 μg), MBP-SirT2 (13 μg), MBP-SirT3(102−399) (28 μg), and SirT5 (13 μg). Reactions were incubated at 30 °C for 2 h and terminated by adding 10% TFA (15 μL). After centrifugation to remove precipitated proteins, the supernatant was analyzed by HPLC using a 50 mM ammonium acetate isocratic system on a Sprite Targa C18 column (40 × 2.1 mm, 5 μm; Higgins Analytical, Inc.). The production of ADP-ribose was quantified using the area of absorption at 260 nm.

Detection of Sirtuin-Catalyzed NAD Hydrolysis by TLC. Reactions were performed in 30 μL volumes with 5 μCi of ^{32}P-NAD, 50 mM Tris-HCl (pH 8.0), 150 mM NaCl, and 10 mM DTT with or without enzymes. Reactions were run for 2 h (except for CD38, which was incubated for 5 min) at 30 °C and quenched with 10% trifluoroacetic acid to a final concentration of 1%. A total of 0.5 μL of each reaction was spotted onto silica gel TLC plates and developed with 70:30 ethanol:2.5 M ammonium acetate. After development, the plates were air-dried and exposed to a phosphorimaging screen. The signal was detected using a STORM860 phosphorimager.

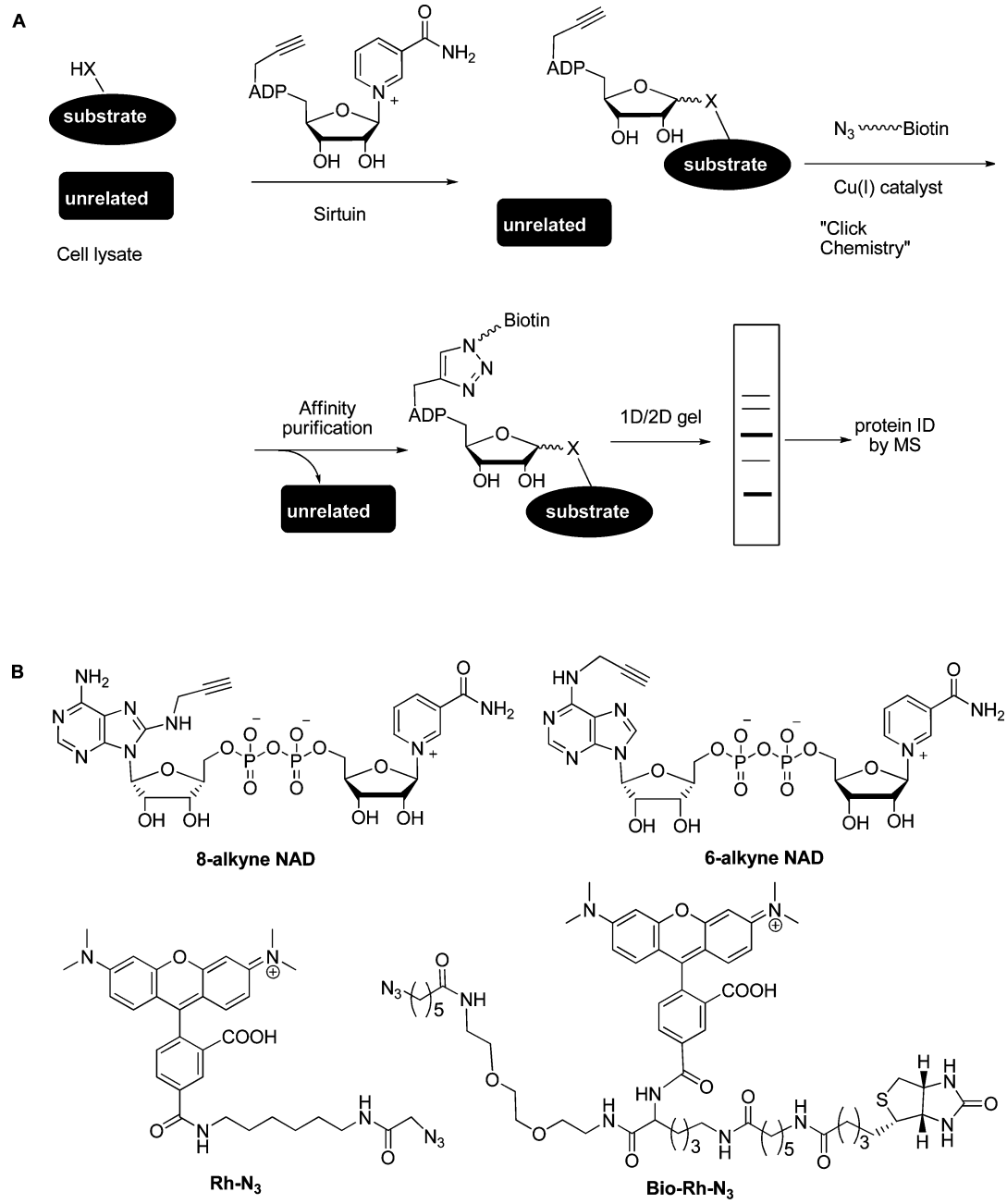

FIGURE 2: (A) Using NAD analogues to label and identify ADP-ribosylated proteins. Purified sirtuin enzymes will be incubated with NAD analogues bearing an alkyne group and cell lysate. Substrate proteins that are ADP-ribosylated with the NAD analogues will then be labeled with an affinity purification tag using click chemistry, isolated, and identified by MS. (B) NAD analogues and purification/detection tags synthesized to label ADP-ribosylation substrates.

RESULTS

The Designed Strategy To Label the ADP-ribosylation Substrates of Sirtuins. To label, isolate, and identify proteins that are ADP-ribosylated by sirtuins, we decided to use NAD analogues bearing an alkyne group on the adenine ring (Figure 2A). After the ADP-ribosyl group is transferred to substrate proteins, purification/detection tags can be introduced using a Cu(I)-catalyzed [3 + 2] cycloaddition reaction between an alkyne group and an azide group, the so-called "click chemistry" (*47, 49, 50*). The major reason for using the click chemistry approach, as opposed to the biotinylated NAD (biotin was attached to the 6 or 8 position of adenine using long linkers) developed by Snyder and co-workers (*51*), is that we think the small alkyne group should minimally perturb the recognition of the NAD analogues by sirtuins. In addition, multiple affinity/detection tags can be used without making more NAD analogues, the syntheses of which are rate-limiting. Using the affinity tag, the substrate proteins can be isolated and then identified by mass spectrometry (MS) (Figure 2A).

DT-Catalyzed eEF-2 ADP-ribosylation Can Be Labeled with 6- and 8-Alkyne NAD. To test the feasibility of the approach, we synthesized two NAD analogues, 6-alkyne NAD and 8-alkyne NAD (Figure 2B). For purification or detection tags, we synthesized a rhodamine-azide compound (Rh-N_3), and a biotin-rhodamine-azide compound (Bio-Rh-N_3). Biotin can be used for affinity purification, while the

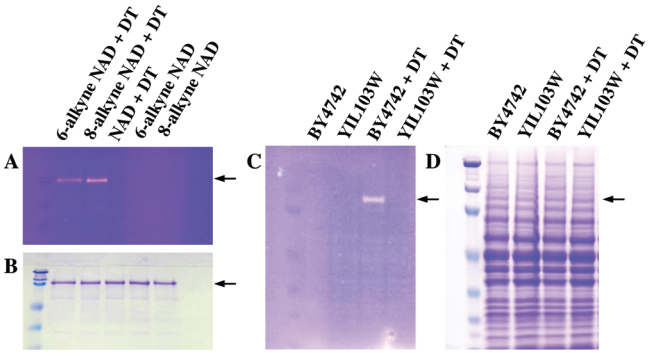

FIGURE 3: Detecting DT-catalyzed ADP-ribosylation with the NAD analogues using purified eEF-2 (A and B) or in crude cell lysate (C and D). The reaction mixture was resolved by SDS−PAGE, and the gel was first visualized under UV (A and C) and then stained with Coomassie blue (B and D). Arrows indicate the position of eEF-2. The BY4742 strain expresses an eEF-2 protein that can be ADP-ribosylated by DT while the YIL103W strain (negative control) expresses an eEF-2 protein that cannot be ADP-ribosylated by DT.

fluorescent rhodamine can be used to detect labeled proteins on gels under ultraviolet (UV) light (*52*).

We first tested the NAD analogues using the ADP-ribosylation of eEF-2 by DT (*38*). Purified yeast eEF-2 and 6- or 8-alkyne NAD (50 μM) were incubated with DT (100 nM) for 30 min at 30 °C. Then, click chemistry was carried out for 30 min at room temperature to attach Rh-N_3 (100 μM). The reaction mixture was then resolved by SDS−PAGE. The gel was first visualized under UV to detect rhodamine fluorescence (Figure 3A), and then stained with Coomassie blue (Figure 3B). The result demonstrates that both 6- and 8-alkyne NAD can label DT-catalyzed eEF-2 ADP-ribosylation. To estimate how efficient the two NAD analogues are as DT substrate, we measured the IC_{50} values of NAD in inhibition of DT-catalyzed eEF-2 labeling using 6- and 8-alkyne NAD. The IC_{50} of NAD inhibiting 6-alkyne NAD in labeling eEF-2 is around 4 μM, while the IC_{50} of NAD inhibiting 8-alkyne NAD in labeling eEF-2 is around 1 μM (Supporting Information, Figure S2).

We next showed that 6-alkyne NAD can label eEF-2 in crude yeast cell lysate under similar labeling conditions. Yeast eEF-2 was labeled with DT in the cell lysate of the wild-type yeast strain BY4742 but was not labeled without DT (Figure 3C). In the lysate of the control strain YIL103W, eEF-2 was not labeled with or without DT (Figure 3C). The YIL103W strain expresses a version of eEF-2 that lacks a posttranslational modification called diphthamide, which is specifically recognized and modified by DT (*53*). Similar labeling was obtained with 8-alkyne NAD (Supporting Information, Figure S3).

Sirtuin-Dependent ADP-ribosylation Cannot Be Labeled with 6- or 8-Alkyne NAD. Our next step is to test whether our NAD analogues can be used to label the ADP-ribosylation substrates of sirtuins. We tested yeast Sir2, human SirT1, mouse SirT4, and mouse SirT6. Both Sir2 and SirT1 have been reported to ADP-ribosylate BSA, histones, and themselves, although it was realized later that the deacetylase activity is responsible for their biological functions. Mouse SirT4 was reported to ADP-ribosylate and regulate the activity of GDH, and no deacetylation substrate has been identified (*36*). For mouse SirT6, when we started to test these NAD analogues, no deacetylation substrate was identified, and it was reported that SirT6 could self-ADP-ribosylate (*35*). We expressed and purified Sir2 and SirT6 with both a His_6 tag and a maltose-binding protein tag at the N-terminus in *E. coli* (designated as MBP-Sir2 and MBP-SirT6). We could not get soluble SirT4 in *E. coli*. Therefore, following the paper that reported the ADP-ribosylation of GDH by SirT4 (*36*), we transiently transfected HeLa cells with a SirT4 expression vector and immunoprecipitated SirT4 from the cell lysate using the Flag tag (Supporting Information, Figure S4). We then tested the NAD analogues in sirtuin-catalyzed ADP-ribosylation. To our disappointment, we did not observe the sirtuin-dependent labeling of histones (Figure 4) or GDH (data not shown).

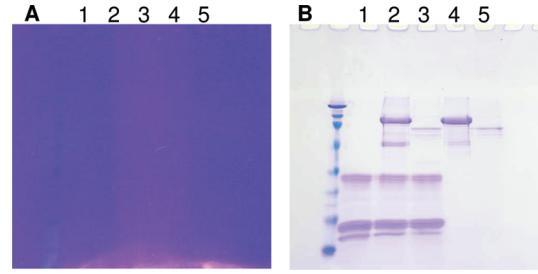

FIGURE 4: Labeling of histone by sirtuin-dependent ADP-ribosylation using 6-alkyne NAD. Calf thymus histones (5 μg) and 6-alkyne NAD (100 μM) were incubated with 3.7 μg of MBP-Sir2 or 1.4 μg of SirT1 for 2 h at 30 °C in 50 mM Tris-HCl (pH 8.0) and 150 mM NaCl. Following incubation with the 6-alkyne NAD, 200 μM Rh-N_3 (in DMF) was added to each sample (10 μL), followed by 600 μM tris[(1-benzyl-1*H*-1,2,3-triazol-4-yl)methyl]-amine (ligand, in DMF), 1.0 mM $CuSO_4$ (in water), and 1.0 mM TCEP (in water). After the click chemistry reaction was allowed to proceed at room temperature for 30 min, the reaction mixture was resolved by SDS−PAGE. (A) The fluorescence image of the protein gel visualized under UV. (B) The protein gel stained with Coomassie blue. Lanes: 1, histone; 2, MBP-Sir2 and histone; 3, SirT1 and histone; 4, MBP-Sir2; 5, SirT1.

Table 1: Kinetic Parameters of NAD and 6-Alkyne NAD as Substrates for Sirtuins

		k_{cat} (s^{-1})	K_m (μM)	k_{cat}/K_m (s^{-1} M^{-1})
MBP-Sir2	NAD	0.083 ± 0.004	130 ± 19	638
	6-alkyne NAD	0.016 ± 0.001	488 ± 70	33
Hst2	NAD	0.064 ± 0.004	7.8 ± 1.7	8205
	6-alkyne NAD	0.006 ± 0.001	110 ± 18	55
SirT1	NAD	0.079 ± 0.003	80 ± 9	988
	6-alkyne NAD	0.122 ± 0.006	183 ± 23	666
MBP-SirT2	NAD	0.021 ± 0.002	46 ± 12	457
	6-alkyne NAD	0.003 ± 0.001	284 ± 30	11
MBP-SirT3	NAD	0.009 ± 0.001	118 ± 13	76
	6-alkyne NAD	0.003 ± 0.001	243 ± 28	12
SirT5	NAD	0.003 ± 0.001	861 ± 245	3.5
	6-alkyne NAD	ND[a]	ND	0.8

[a] ND: not determined because the reaction rate is linear with 6-alkyne NAD concentration even at the highest concentration tested (750 μM).

6-Alkyne NAD Is a Substrate for Sirtuin's Deacetylase Activity. We thought of two possible reasons why the NAD analogues failed to label the ADP-ribosylation substrates of sirtuins. One is that the sirtuins we obtained are not active. The other is that the NAD analogues are not substrates of sirtuins. We ruled out both possibilities by testing sirtuin-catalyzed deacetylation of histone peptides (Table 1). Using an HPLC assay, we found that MBP-Sir2 can deacetylate histone H3AcK9 (residue 4−15) with a k_{cat} value of 0.083 ± 0.004 s^{-1} and a K_m value of 130 ± 19 μM for NAD. Both 6- and 8-alkyne NAD are substrates for MBP-Sir2,

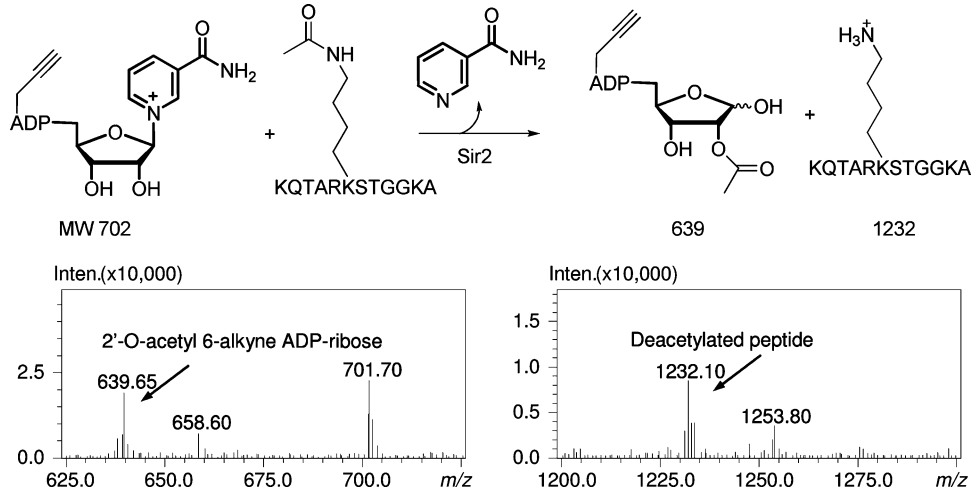

FIGURE 5: 6-Alkyne NAD is a substrate for the deacetylase activity of sirtuins. The structures of the reaction products are shown on top. At the bottom are MS spectra showing the formation of 2′-*O*-acetyl 6-alkyne ADP-ribose and the deacetylated peptide using 6-alkyne NAD as a cosubstrate and MBP-Sir2 as the deacetylase. Several other sirtuins were also tried, and similar results were obtained.

although 6-alkyne NAD is better (data not shown). Therefore, further studies were focused on 6-alkyne NAD. Using LCMS, the formation of 2′-*O*-acetyl 6-alkyne ADP-ribose and the deacetylated peptide can be detected (Figure 5). To further characterize the efficiency of 6-alkyne NAD as a sirtuin substrate, we measured the k_{cat} and K_m values of MBP-Sir2 on 6-alkyne NAD. The k_{cat} is 0.016 ± 0.001 s^{-1}, and K_m is 488 ± 70 μM. Compared with using NAD as a substrate, the catalytic efficiency (k_{cat}/K_m) of MBP-Sir2 with 6-alkyne NAD as a substrate is ~19-fold lower. We also tested 6-alkyne NAD with yeast Hst2, human SirT1, SirT2, SirT3, and SirT5. Similarly, 6-alkyne NAD is a substrate for all of these sirtuin deacetylation reactions, albeit with lower catalytic efficiency compared with NAD (Table 1). For SirT1, the catalytic efficiency of 6-alkyne NAD is similar to NAD. For yeast Hst2, the catalytic efficiency is about 100-fold lower, but this is probably due to the fact that Hst2 has a particularly small K_m on NAD compared with other sirtuins.

Sirtuin-Dependent ADP-ribosylation is 3−4 Orders of Magnitude Weaker Compared with a Well-Established Enzymatic ADP-ribosylation Reaction. The fact that our NAD analogues are deacetylation substrates but failed to label ADP-ribosylation substrates of sirtuins suggests that the ADP-ribosyltransferase activity of sirtuins may be very weak. To gain further insight on the ADP-ribosyltransferase activity, we carried out ADP-ribosylation assays with ^{32}P-NAD for MBP-Sir2 and SirT1. Consistent with reported results, we indeed observed sirtuin-dependent ADP-ribosylation of histones (Figure 6A). MBP-Sir2 and SirT1 increased the ADP-ribosylation of histones approximately 3- and 5-fold, respectively, compared with control. However, when we compare the sirtuin-dependent ADP-ribosylation of histones with the DT-catalyzed ADP-ribosylation of eEF-2, the ADP-ribosylation of histones is very weak (Figure 6B; note the enormous amount of labeling on eEF-2 in lane 4). If we assume eEF-2 is quantitatively ADP-ribosylated by DT, the amount of histones or MBP-Sir2 labeled is estimated to be less than 0.5% of the total histones or MBP-Sir2 in the reactions. By estimation, the observed rate constant, k_{obs} (rate/([sirtuin][NAD])), of MBP-Sir2 (1 s^{-1} M^{-1}) or SirT1 (2 s^{-1} M^{-1}) is more than 5000-fold lower than that of DT (1×10^4 s^{-1} M^{-1}). Comparing with the k_{cat}/K_m values of MBP-Sir2 or SirT1 catalyzed deacetylation, MBP-Sir2 or SirT1 catalyzed ADP-ribosylation is ~500-fold weaker. Thus, sirtuin self-ADP-ribosylation and sirtuin-dependent ADP-ribosylation of histones are very weak.

Free ADP-ribose Can Covalently Modify Histones. The weak ADP-ribosylation activity of sirtuins prompted us to ask whether the reaction can result from nonenzymatic ADP-ribosylation by ADP-ribose or 2′-*O*-acetyl ADP-ribose. Thus we compared the labeling of histones with ^{32}P-ADP-ribose and ^{32}P-NAD. We generated ^{32}P-ADP-ribose from ^{32}P-NAD by incubating ^{32}P-NAD with the NAD glycohydrolase CD38 (*54*−*60*) (10 nM) for 5 min before adding histones. Incubation of 5 μM cold NAD with 10 nM CD38 confirmed that 5 min incubation with CD38 is sufficient to convert essentially all of the ^{32}P-NAD to ^{32}P-ADP-ribose (Figure 6C). The result shown in Figure 6D suggests that indeed ADP-ribose can label histones better than NAD by about 3-fold. Given that 2′-*O*-acetyl ADP-ribose should have similar reactivity to ADP-ribose in nonenzymatic reactions, the data suggest that sirtuin-dependent ADP-ribosylation could result from nonenzymatic ADP-ribosylation with the 2′-*O*-acetyl ADP-ribose generated in deacetylation reactions, as recently suggested by Denu and co-workers (*61*). This mechanism could be a major pathway for sirtuins that have strong deacetylase activity. In support of this, we monitored the production of ADP-ribose or 2′-*O*-acetyl ADP-ribose on sirtuin-dependent ADP-ribosylation reaction with ^{32}P-NAD by TLC. Indeed, at the end of the reaction, almost all NAD is converted to 2′-*O*-acetyl ADP-ribose (Supporting Information, Figure S5).

Sirtuins Can Promote the Hydrolysis of NAD in the Absence of Deacetylation Substrates. The above results suggest a possible nonenzymatic mechanism for sirtuin-dependent ADP-ribosylation reactions. However, this mechanism may not apply to sirtuins that have no deacetylation activity detected yet, such as SirT4, or for sirtuins known to have deacetylation activity but in the absence of acetyl Lys substrate. We thought that this problem can be addressed if sirtuins can catalyze the hydrolysis of NAD to generate ADP-ribose in the absence of an acetyl peptide substrate. Indeed, such activity has been reported for *Plasmodium falciparum* Sir2 (*62*). In order to find out whether the nonenzymatic ADP-ribosylation mechanism with sirtuin-generated ADP-ribose could be operating, we tested whether yeast and

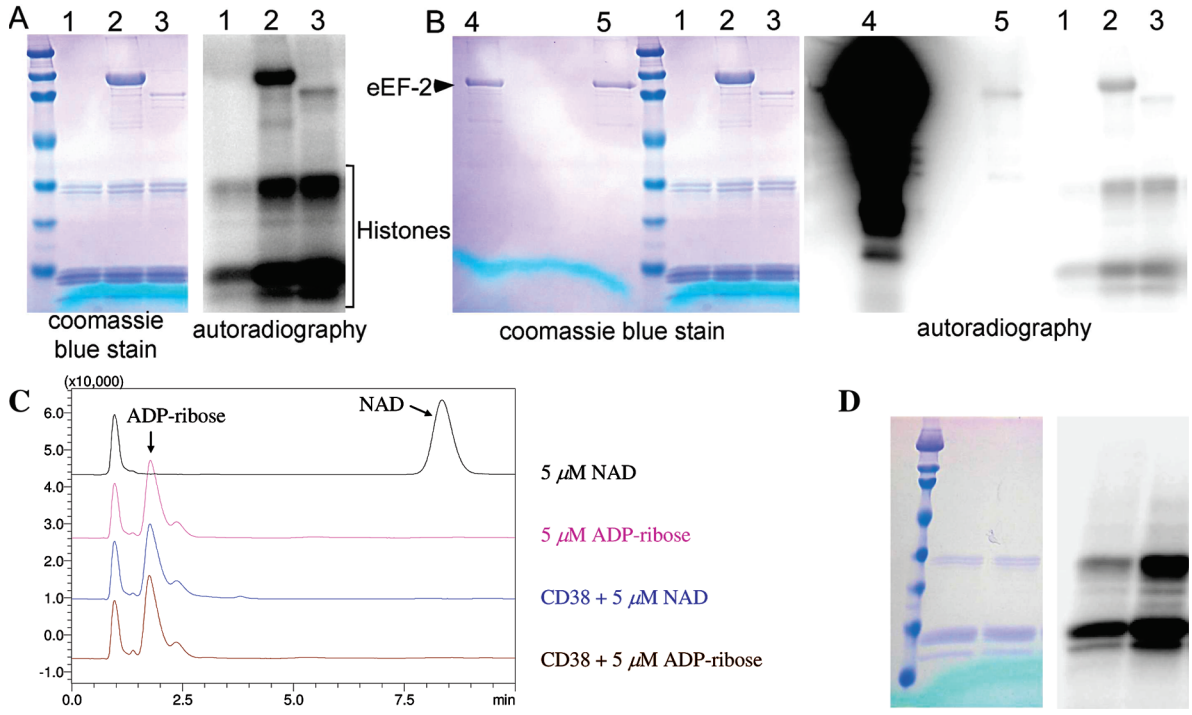

FIGURE 6: Sirtuin-dependent ADP-ribosylation is very weak. (A) 5.0 μg of calf thymus histones was incubated with 5 μCi of ^{32}P-NAD without sirtuins (lane 1), with 3.7 μg of MBP-Sir2 (lane 2), or with 1.4 μg of SirT1 (lane 3) for 2 h. (B) Comparison of the sirtuin-dependent histone ADP-ribosylation to DT-catalyzed eEF-2 ADP-ribosylation. Lanes 1−3 are the same as in (A). Lane 4 is 2.0 μg of eEF-2 ADP-ribosylated in the presence of 100 nM DT; lane 5 is 2.0 μg of eEF-2 without DT. Note that the gel shown in (A) is actually part of the gel shown in (B) with enhanced contrast to better show sirtuin-dependent ADP-ribosylation. (C) HPLC traces showing that CD38 (10 nM) can convert essentially all NAD (5 μM) molecules to ADP-ribose in 5 min. (D) Comparison of the ADP-ribosylation of histones with ^{32}P-ADP-ribose and ^{32}P-NAD. Using CD38 (10 nM), ^{32}P-NAD (5 μCi) was converted to ^{32}P-ADP-ribose, and then this reaction mixture was used to ADP-ribosylate histones. The left picture shows the Coomassie blue-stained gel, and the right picture shows the autoradiograph. The left lane is the labeling reaction without CD38 treatment; the right lane is the labeling reaction with CD38 treatment. The labeling result suggests that ADP-ribose can react with proteins nonenzymatically.

mammalian sirtuins also have this NAD glycohydrolase activity in the absence of acetyl peptides as deacetylation substrates. The results for SirT1 and yeast Sir2 shown in Figure 7 suggest they can promote the hydrolysis of NAD. Other sirtuins tested (SirT2, MBP-SirT3, and SirT5) gave similar results (data not shown). The NAD hydrolysis activity of sirtuins is consistent with the SIRT5 structures recently reported by Schuetz et al. (*25*). In one of the reported structures, ADP-ribose was cocrystallized when NAD was added to the SIRT5 protein during crystallization.

However, the NAD hydrolysis activity of sirtuins in the absence of acetyl peptide is not strong enough to explain the observed sirtuin-dependent ADP-ribosylation. With the conditions we used, only about 1% of the total NAD (200 μM) is hydrolyzed. The estimated k_{obs} is on the order of 1 s^{-1} M^{-1}, about 2−3 orders of magnitude lower than the deacetylation activity of most sirtuins (Table 1). When we lower the NAD concentration to 5 μM, which we think is closer to the ^{32}P-NAD concentration used in the ADP-ribosylation reactions, the amount of ADP-ribose generated in 2 h was barely detectable (Supporting Information, Figure S6). As shown in Figure 6, CD38, which can completely hydrolyze 5 μM NAD in 5 min, only increased the ADP-ribosylation about 3-fold. Thus, the NAD glycohydrolase activity of sirtuins and nonenzymatic ADP-ribosylation with ADP-ribose should not be the major contribution of the observed ADP-ribosylation activity of sirtuins. This argues that the ADP-ribosylation activity of sirtuins in the absence of a deacetylation substrate is mostly via enzymatic mechanisms, as will be further discussed below.

DISCUSSION

Possible Mechanisms for Sirtuin-Dependent ADP-ribosylation and the Relative Contribution of Different Mechanisms. Sirtuins have been well-known for their NAD-dependent deacetylation activity. However, many sirtuins have been reported to harbor ADP-ribosyltransferase activity as well (*34*−*36*, *63*). Based on the established NAD-dependent deacetylation reaction mechanism, several ADP-ribosylation mechanisms can be proposed. One mechanism is similar to the first step of the deacetylation mechanism, which involves the attack of the 1′ position of NAD by a nucleophilic residue from substrate proteins (mechanism A in Figure 8). Our work on several yeast and mammalian sirtuins and the work of Sauve and co-workers on *P. falciparum* Sir2 showed that, in the absence of deacetylation substrates, sirtuins can catalyze the transfer of ADP-ribosyl group to water or methanol to generate the α-ADP-ribosyl product, with water/methanol presumably occupying the site where acetyl peptide normally occupies. One can imagine that nucleophilic side chains of some proteins can similarly occupy the site and thus result in protein ADP-ribosylation. The second mechanism is that the alkylimidate intermediate formed in the deacetylation reaction can be captured by nucleophilic residues of proteins, resulting in protein ADP-ribosylation (mechanism B in Figure 8). Both mechanism

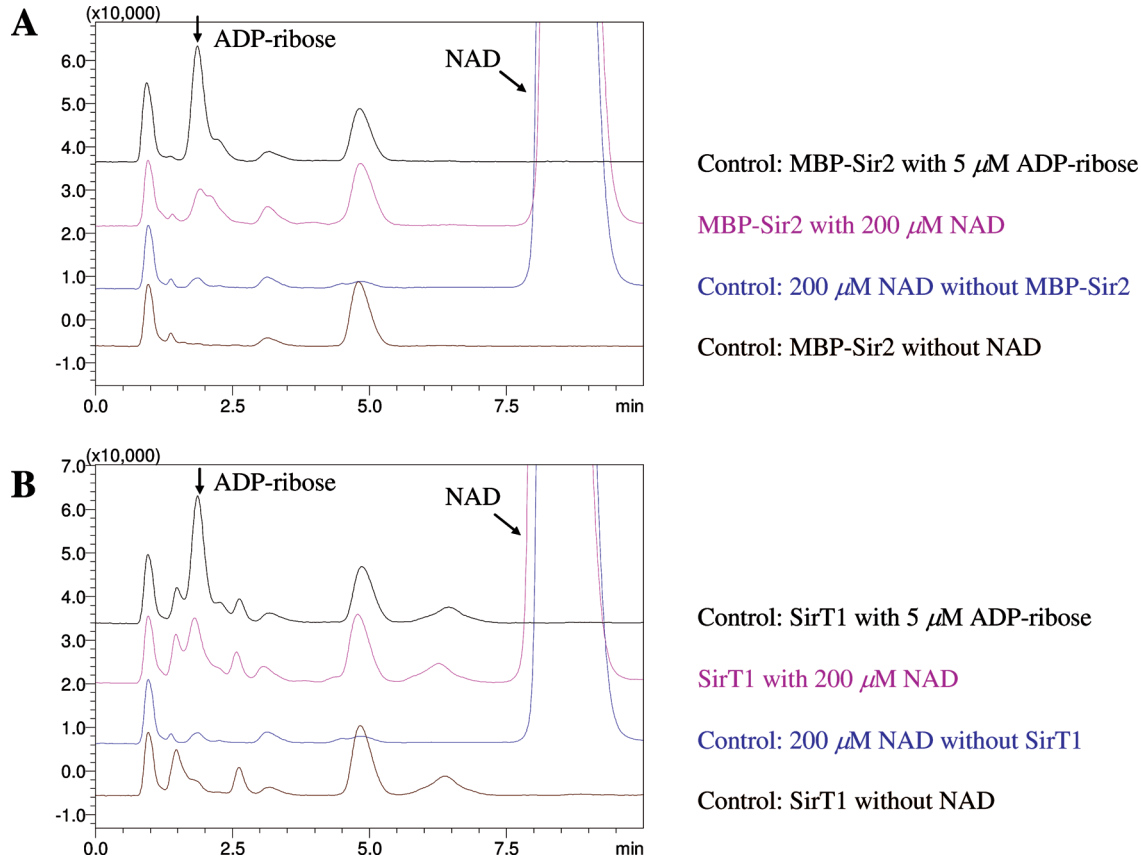

FIGURE 7: Sirtuins can promote NAD hydrolysis in the absence of deacetylation substrates. HPLC traces for MBP-Sir2 (20.0 μg) and SirT1 (10.0 μg) catalyzed NAD hydrolysis are shown with different control reactions in 20 mM Tris-HCl buffer, pH 7.5. NAD concentration was 200 μM. Three controls were used: the same reaction without NAD, the same reaction without sirtuin, and the same reaction without NAD but spiked with 5 μM ADP-ribose.

A and mechanism B are the direct consequence of sirtuin's catalytic action, and thus we call them "enzymatic ADP-ribosylation". In contrast, two mechanisms that are the indirect consequence of sirtuin's enzymatic action can also be proposed. One mechanism is that the 2′-*O*-acetyl ADP-ribose generated in deacetylation reactions can nonspecifically react with nucleophilic residues such as Lys and Cys (Figure 8, mechanism C). Similarly, in the absence of deacetylation substrates, sirtuins can also generate ADP-ribose, which can also react with proteins nonenzymatically (Figure 8, mechanism D).

We found that ADP-ribose can label histones (Figure 6D). Similarly, Denu and co-workers found that 2′-*O*-acetyl ADP-ribose can label histones (*61*). NAD-dependent deacetylation reactions will generate 2′-*O*-acetyl ADP-ribose. For sirtuins with strong deacetylation activity, such as yeast Sir2 and human SirT1, 2′-*O*-acetyl ADP-ribose can be generated very quickly, and therefore this nonenzymatic pathway can be a major contribution to the observed ADP-ribosylation activity.

For sirtuins with no deacetylation activity detected yet, however, this nonenzymatic pathway cannot operate. Sauve and co-workers (*62*) suggest that ADP-ribose can be generated by sirtuins in the absence of deacetylation. We tested several mammalian sirtuins to see whether they can hydrolyze NAD and therefore ADP-ribosylate proteins nonenzymatically with ADP-ribose. Indeed, all mammalian and yeast sirtuins tested can promote the hydrolysis of NAD. However, the rate is very slow. By comparing with the result obtained with CD38, which can convert 5 μM NAD to ADP-ribose in 5 min but only increased the ADP-ribosylation several fold in 2 h, we think this mechanism can only account for a very small portion of the sirtuin-dependent ADP-ribosylation observed. This result suggests that enzymatic ADP-ribosylation mechanisms (Figure 8, mechanisms A and B) must be the major pathways for the ADP-ribosylation activity of sirtuins with no deacetylation activity detected.

Of these two potential ADP-ribosylation mechanisms, which one could be the major pathway for sirtuin-dependent ADP-ribosylation? This will depend on the exact conditions that the reactions are carried out. In the absence of acetyl peptides, of course mechanism A will be the one operating. However, in the presence of acetyl peptides, we think it is likely mechanism B, which is dependent on the imidate intermediate formed in the deacetylation reaction. This conclusion is based on several recent reports by Denu and Sauve. Denu and co-workers showed that, for *Trypanosoma brucei* Sir2, mechanism B is the major pathway (*61*). For *P. falciparum* Sir2, when acetyl peptides were added to the reaction, the formation of the α-ADP-ribosyl product was suppressed and the formation of β-ADP-ribosyl product dominated (*62*). Since mechanism A gives α-ADP-ribosyl product while mechanism B gives β-ADP-ribosyl product, this result suggests that, for *P. falciparum* Sir2, mechanism B is also the predominant enzymatic ADP-ribosylation mechanism when acetyl peptide is present.

The ADP-ribosylation Activity of Sirtuins May Not Be Physiologically Relevant. Our data showed that the ADP-ribosylation activity of several sirtuins is >1000-fold slower than DT or their deacetylation activity. This is consistent with the recent report by Denu and co-workers that the ADP-

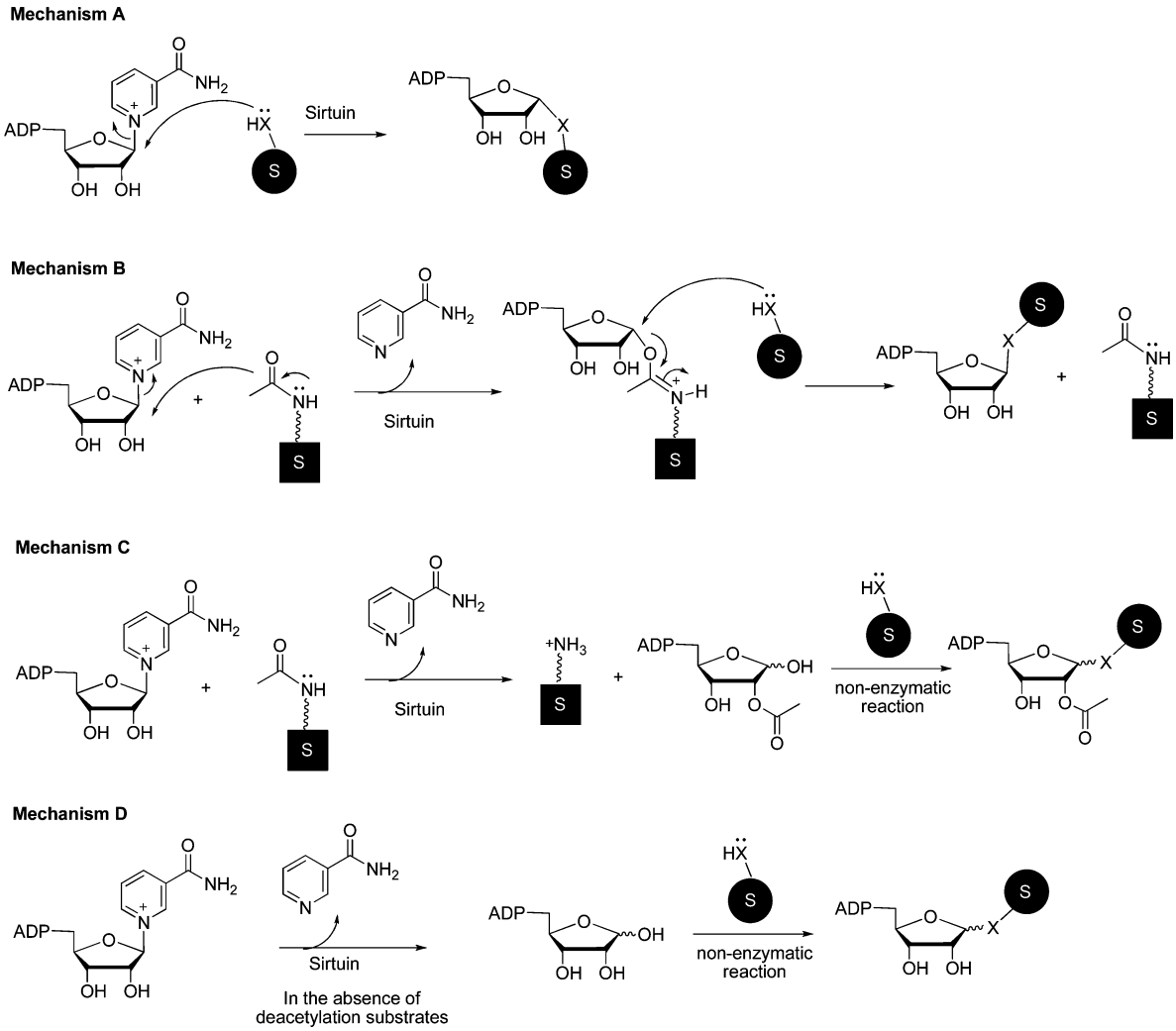

FIGURE 8: Four possible mechanisms for sirtuin-dependent ADP-ribosylation. Mechanisms A and B can be considered enzymatic ADP-ribosylation, while mechanisms C and D are nonenzymatic ADP-ribosylation with either 2′-*O*-acetyl ADP-ribose or ADP-ribose generated by sirtuin.

ribosylation activity of *T. brucei* Sir2 is 5 orders of magnitude slower compared with its deacetylation activity. Below we propose a model to explain why sirtuin-dependent ADP-ribosylation is weak and may not be physiologically relevant.

Based on well-accepted NAD-dependent deacetylation mechanism, the formation of the imidate intermediate is much faster than the next step, the nucleophilic attack of the 2′-OH that ultimately leads to deacetylation (Figure 9, pathway a). The imidate intermediate can go in several different competitive pathways: reaction with nicotinamide to re-form NAD and the original acetyl peptide (Figure 9, pathway b), reaction with water to form ADP-ribose and the original acetyl peptide (Figure 9, pathway c), and reaction with nucleophilic groups on proteins to give ADP-ribosylated protein and the original acetyl peptide (Figure 9, pathway d). For sirtuins with strong deacetylation activity, the reaction with nicotinamide is the fastest, followed by the forward reaction that leads to deacetylation, while the competing reactions with water/methanol or nucleophilic groups on proteins are much slower. However, the contribution of different reaction pathways could change in different conditions. For example, when the catalytic His residue in the Hst2 active site is mutated to Ala (*17*), more reaction product with water/methanol can form because the forward deacetylation reaction is now much slower without the general base to deprotonate the 2′-OH. Another situation is when the acetyl peptide is not an efficient substrate for deacetylation, such as the acetyl peptides used for *P. falciparum* Sir2-catalyzed reaction (*62*). The k_{cat} obtained for *P. falciparum* Sir2 is about 100-fold lower than the k_{cat} obtained for other sirtuins, such as yeast Sir2 used in this study. We think this is likely the reason why the ADP-ribosyl transfer to water/methanol is much more appreciable for *P. falciparum* Sir2. Therefore, using acetyl peptides that are not good substrates for deacetylation could in principle increase the portion of NAD that goes to the ADP-ribosylation reaction via mechanism B in Figure 8. However, the absolute rate of ADP-ribosylation is limited because the sirtuin active site is optimized for binding of nicotinamide but not other nucleophiles. We argue that this is why no strong sirtuin-dependent ADP-ribosylation has been observed so far.

To date, the only sirtuin-catalyzed ADP-ribosylation that is reported to have a physiological function is SirT4-catalyzed GDH ADP-ribosylation (*36*). Due to the difficulty in the expression and purification of mammalian SirT4, we did not get enough purified SirT4 protein to carry out the ^{32}P-NAD labeling as we did for MBP-Sir2 and SirT1. However, based on the autoradiograph shown in the two papers that reported the ADP-ribosylation activity of SirT4 (*36, 63*), the labeling

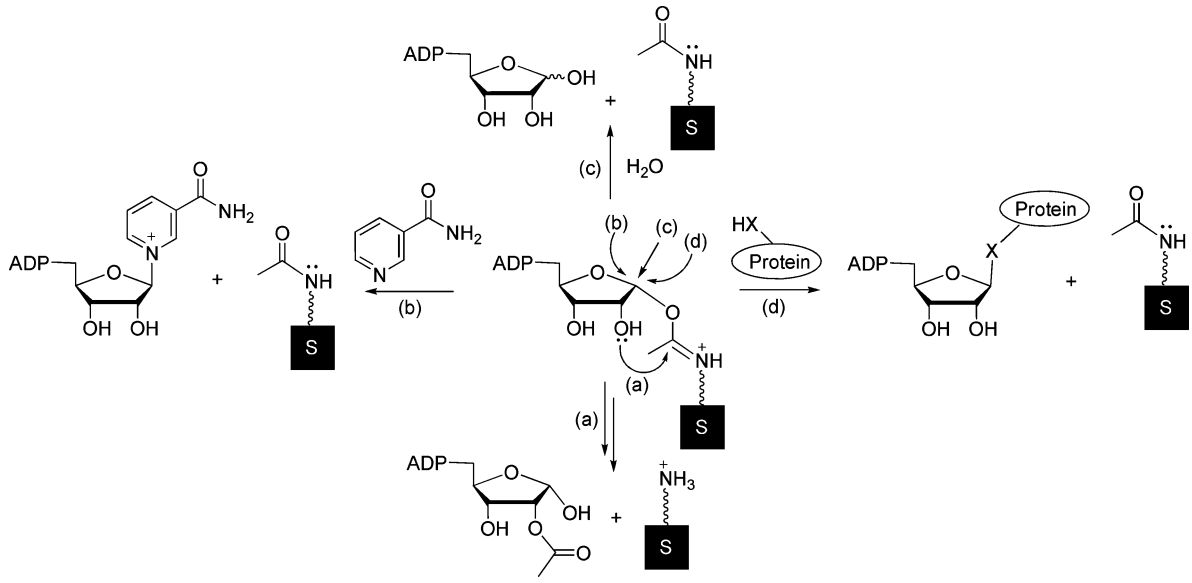

FIGURE 9: A common intermediate can explain the different activities of sirtuins. The imidate intermediate formed in the presence of an acetyl peptide can undergo different pathways depending on the attacking nucleophiles. The fastest pathway is the reaction with nicotinamide (b), which gives back the starting NAD and acetyl peptide (reverse reaction). With the right acetyl peptide substrate, the deacetylation pathway (a) is the major forward pathway, while the ADP-ribosylation pathways (c and d) constitute a tiny fraction of the total forward reactions. However, when (a) is inefficient due to mutations in sirtuins or thhe wrong acetyl peptide substrate, the contribution of pathways c and d can increase. However, the absolute rates of pathways c and d are always very small, and thus no strong ADP-ribosylation activity has been detected.

intensity is similar to the histone ADP-ribosylation promoted by MBP-Sir2 and SirT1. Thus, the ADP-ribosylation activity of SirT4 is likely also very weak, and its physiological relevance should be further investigated. SirT4 may indeed be a protein ADP-ribosyltransferase, but the true physiological ADP-ribosylation substrate of SirT4 is yet to be discovered. An alternative explanation, which we think is more likely, is that the biological function of SirT4 is mediated by its deacetylation activity. The reason why no deacetylation activity has been detected for SirT4 could be that it has very strict deacetylation substrate specificity. A recent paper by Chua and co-workers showed that this is the case for SirT6 (*64*). SirT6 was postulated to be an ADP-ribosyltransferase because no deacetylation substrates were identified and it can self-ADP-ribosylate (*35*). Chua and co-workers showed that SirT6 selectively deacetylates a histone H3 K9 acetyl peptide, but not other acetyl peptides tested (*64*). It is possible that SirT4 is also a deacetylase with strict substrate specificity like SirT6.

The Advantage and Disadvantage of Using ^{32}P-NAD and NAD Analogues To Detect Protein ADP-ribosylation. The field of ADP-ribosylation has a long history of false enzymatic or nonphysiological ADP-ribosylation reactions. For example, glyceraldehyde-3-phosphate dehydrogenase (GAPDH) was thought to be ADP-ribosylated in response to nitric oxide, which turned out to be a noncovalent modification (*65*). Actin was found to be nonenzymatically ADP-ribosylated presumably by reacting with free ^{32}P-ADP-ribose contamination in ^{32}P-NAD (*66, 67*). Earlier studies that proposed the existence of endogenous enzymatic protein ADP-ribosylation on Cys residues were also thought to be nonenzymatic in many cases (*67*). Another example is the ADP-ribosylation of eEF-2. After the discovery that diphtheria toxin can ADP-ribosylate eEF-2 on diphthamide residue, several reports suggest that eukaryotic cells have an endogenous ADP-ribosyltransferase that can modify eEF-2 (*68*−*70*). Interestingly, one paper reported the attempted purification of this putative eEF-2 ADP-ribosyltransferase and found that it was eEF-2 itself (*71*). Based on the result shown in Figure 6B, indeed eEF-2 can be self-ADP-ribosylated. However, the intensity is several hundred-fold weaker compared to the diphtheria toxin-catalyzed ADP-ribosylation. Thus the reported ADP-ribosylation of eEF-2 by endogenous enzymes is likely not physiologically significant either. Similarly, it was reported that CD38 can ADP-ribosylate other proteins such as BSA (*72*). Given our result shown in Figure 6, this can be attributed to the nonenzymatic reaction with the ADP-ribose generated. For sirtuin-dependent ADP-ribosylation, given that the activity is very weak and the presence of the nonenzymatic ADP-ribosylation pathways, the interpretation of the sirtuin-dependent ADP-ribosylation must be carried out with caution.

Given that nonphysiological ADP-ribosylation is frequently observed with ^{32}P-NAD, caution must be used when analyzing ADP-ribosylation reactions using ^{32}P-NAD. Considering this, our alkyne-tagged NAD molecules may offer advantages and complement the use of ^{32}P-NAD in detecting robust and physiologically relevant enzymatic ADP-ribosylation because these NAD analogues do not detect weak (and likely not physiologically relevant) ADP-ribosylation reactions. Our laboratory is currently exploring these NAD analogues on other mammalian ADP-ribosyltransferases, including poly(ADP-ribose) polymerases (PARPs) and mono(ADP-ribosyl)transferases (ARTs).

ACKNOWLEDGMENT

We thank Dr. Jon Collier (Harvard Medical School) for providing DT plasmid, Dr. Marcia Haigis (Harvard Medical School) for providing SirT4 plasmid, and Dr. Quan Hao (previously Cornell MacCHESS, now University of Hong

Kong) and Dr. Hon Cheung Lee (University of Hong Kong) for providing CD38.

SUPPORTING INFORMATION AVAILABLE

Figures showing the synthesis of NAD analogues, IC_{50} measurement, labeling of yeast cell lysate with 8-alkyne NAD, expression of sirtuins, NMR assignments of NAD analogues, TLC analysis of sirtuin-dependent ADP-ribosylation reactions with ^{32}P-NAD, and HPLC analysis of sirtuin-promoted NAD hydrolysis at 5 μM NAD concentration. This material is available free of charge via the Internet at http://pubs.acs.org.

REFERENCES

1. Sauve, A. A., Wolberger, C., Schramm, V. L., and Boeke, J. D. (2006) The Biochemistry of Sirtuins. *Annu. Rev. Biochem. 75*, 435–465.
2. Michan, S., and Sinclair, D. (2007) Sirtuins in Mammals: Insights into Their Biological Function. *Biochem. J. 404*, 1–13.
3. Imai, S.-i., Armstrong, C. M., Kaeberlein, M., and Guarente, L. (2000) Transcriptional Silencing and Longevity Protein Sir2 Is an NAD-Dependent Histone Deacetylase. *Nature 403*, 795–800.
4. Zhao, W., Kruse, J.-P., Tang, Y., Jung, S. Y., Qin, J., and Gu, W. (2008) Negative Regulation of the Deacetylase SIRT1 by DBC1. *Nature 451*, 587–590.
5. Heltweg, B., Gatbonton, T., Schuler, A. D., Posakony, J., Li, H., Goehle, S., Kollipara, R., DePinho, R. A., Gu, Y., Simon, J. A., and Bedalov, A. (2006) Antitumor Activity of a Small-Molecule Inhibitor of Human Silent Information Regulator 2 Enzymes. *Cancer Res. 66*, 4368–4377.
6. Outeiro, T. F., Kontopoulos, E., Altmann, S. M., Kufareva, I., Strathearn, K. E., Amore, A. M., Volk, C. B., Maxwell, M. M., Rochet, J.-C., McLean, P. J., Young, A. B., Abagyan, R., Feany, M. B., Hyman, B. T., and Kazantsev, A. G. (2007) Sirtuin 2 Inhibitors Rescue α-Synuclein-Mediated Toxicity in Models of Parkinson's Disease. *Science 317*, 516–519.
7. Guarente, L. (2006) Sirtuins as Potential Targets for Metabolic Syndrome. *Nature 444*, 868–874.
8. Milne, J. C., Lambert, P. D., Schenk, S., Carney, D. P., Smith, J. J., Gagne, D. J., Jin, L., Boss, O., Perni, R. B., Vu, C. B., Bemis, J. E., Xie, R., Disch, J. S., Ng, P. Y., Nunes, J. J., Lynch, A. V., Yang, H., Galonek, H., Israelian, K., Choy, W., Iffland, A., Lavu, S., Medvedik, O., Sinclair, D. A., Olefsky, J. M., Jirousek, M. R., Elliott, P. J., and Westphal, C. H. (2007) Small Molecule Activators of SIRT1 as Therapeutics for the Treatment of Type 2 Diabetes. *Nature 450*, 712–716.
9. Lagouge, M., Argmann, C., Gerhart-Hines, Z., Meziane, H., Lerin, C., Daussin, F., Messadeq, N., Milne, J., Lambert, P., Elliott, P., Geny, B., Laakso, M., Puigserver, P., and Auwerx, J. (2006) Resveratrol Improves Mitochondrial Function and Protects against Metabolic Disease by Activating SIRT1 and PGC-1[alpha]. *Cell 127*, 1109–1122.
10. Baur, J. A., Pearson, K. J., Price, N. L., Jamieson, H. A., Lerin, C., Kalra, A., Prabhu, V. V., Allard, J. S., Lopez-Lluch, G., Lewis, K., Pistell, P. J., Poosala, S., Becker, K. G., Boss, O., Gwinn, D., Wang, M., Ramaswamy, S., Fishbein, K. W., Spencer, R. G., Lakatta, E. G., Le Couteur, D., Shaw, R. J., Navas, P., Puigserver, P., Ingram, D. K., de Cabo, R., and Sinclair, D. A. (2006) Resveratrol Improves Health and Survival of Mice on a High-Calorie Diet. *Nature 444*, 337–342.
11. Howitz, K. T., Bitterman, K. J., Cohen, H. Y., Lamming, D. W., Lavu, S., Wood, J. G., Zipkin, R. E., Chung, P., Kisielewski, A., Zhang, L.-L., Scherer, B., and Sinclair, D. A. (2003) Small Molecule Activators of Sirtuins Extend *Saccharomyces cerevisiae* Lifespan. *Nature 425*, 191–196.
12. Tanner, K. G., Landry, J., Sternglanz, R., and Denu, J. M. (2000) Silent Information Regulator 2 Family of NAD-Dependent Histone/Protein Deacetylases Generates a Unique Product, 1-O-Acetyl-ADP-ribose. *Proc. Natl. Acad. Sci. U.S.A. 97*, 14178–14182.
13. Tanny, J. C., and Moazed, D. (2001) Coupling of Histone Deacetylation to NAD Breakdown by the Yeast Silencing Protein Sir2: Evidence for Acetyl Transfer from Substrate to an NAD Breakdown Product. *Proc. Natl. Acad. Sci. U.S.A. 98*, 415–420.
14. Sauve, A. A., Celic, I., Avalos, J., Deng, H., Boeke, J. D., and Schramm, V. L. (2001) Chemistry of Gene Silencing: The Mechanism of NAD$^+$-Dependent Deacetylation Reactions. *Biochemistry 40*, 15456–15463.
15. Jackson, M. D., and Denu, J. M. (2002) Structural Identification of 2′- and 3′-O-Acetyl-ADP-ribose as Novel Metabolites Derived from the Sir2 Family of beta-NAD$^+$-Dependent Histone/Protein Deacetylases. *J. Biol. Chem. 277*, 18535–18544.
16. Jackson, M. D., Schmidt, M. T., Oppenheimer, N. J., and Denu, J. M. (2003) Mechanism of Nicotinamide Inhibition and Transglycosidation by Sir2 Histone/Protein Deacetylases. *J. Biol. Chem. 278*, 50985–50998.
17. Smith, B. C., and Denu, J. M. (2006) Sir2 Protein Deacetylases: Evidence for Chemical Intermediates and Functions of a Conserved Histidine. *Biochemistry 45*, 272–282.
18. Smith, B. C., and Denu, J. M. (2007) Sir2 Deacetylases Exhibit Nucleophilic Participation of Acetyl-Lysine in NAD$^+$ Cleavage. *J. Am. Chem. Soc. 129*, 5802–5803.
19. Sauve, A. A., and Schramm, V. L. (2003) Sir2 Regulation by Nicotinamide Results from Switching between Base Exchange and Deacetylation Chemistry. *Biochemistry 42*, 9249–9256.
20. Avalos, J. L., Celic, I., Muhammad, S., Cosgrove, M. S., Boeke, J. D., and Wolberger, C. (2002) Structure of a Sir2 Enzyme Bound to an Acetylated p53 Peptide. *Mol. Cell 10*, 523–535.
21. Chang, J.-H., Kim, H.-C., Hwang, K.-Y., Lee, J.-W., Jackson, S. P., Bell, S. D., and Cho, Y. (2002) Structural Basis for the NAD-Dependent Deacetylase Mechanism of Sir2. *J. Biol. Chem. 277*, 34489–34498.
22. Min, J., Landry, J., Sternglanz, R., and Xu, R.-M. (2001) Crystal Structure of a SIR2 Homolog-NAD Complex. *Cell 105*, 269–279.
23. Zhao, K., Chai, X., and Marmorstein, R. (2003) Structure of the Yeast Hst2 Protein Deacetylase in Ternary Complex with 2′-O-Acetyl ADP Ribose and Histone Peptide. *Structure 11*, 1403–1411.
24. Finnin, M. S., Donigian, J. R., and Pavletich, N. P. (2001) Structure of the Histone Deacetylase SIRT2. *Nat. Struct. Mol. Biol. 8*, 621–625.
25. Schuetz, A., Min, J., Antoshenko, T., Wang, C.-L., Allali-Hassani, A., Dong, A., Loppnau, P., Vedadi, M., Bochkarev, A., Sternglanz, R., and Plotnikov, A. N. (2007) Structural Basis of Inhibition of the Human NAD$^+$-Dependent Deacetylase SIRT5 by Suramin. *Structure 15*, 377–389.
26. Zhao, K., Chai, X., and Marmorstein, R. (2004) Structure and Substrate Binding Properties of cobB, a Sir2 Homolog Protein Deacetylase from *Escherichia coli*. *J. Mol. Biol. 337*, 731–741.
27. Hoff, K. G., Avalos, J. L., Sens, K., and Wolberger, C. (2006) Insights into the Sirtuin Mechanism from Ternary Complexes Containing NAD$^+$ and Acetylated Peptide. *Structure 14*, 1231–1240.
28. Sanders, B. D., Zhao, K., Slama, J. T., and Marmorstein, R. (2007) Structural Basis for Nicotinamide Inhibition and Base Exchange in Sir2 Enzymes. *Mol. Cell 25*, 463–472.
29. Zhao, K., Harshaw, R., Chai, X., and Marmorstein, R. (2004) Structural Basis for Nicotinamide Cleavage and ADP-ribose Transfer by NAD$^+$-Dependent Sir2 Histone/Protein Deacetylases. *Proc. Natl. Acad. Sci. U.S.A. 101*, 8563–8568.
30. Hawse, W. F., Hoff, K. G., Fatkins, D. G., Daines, A., Zubkova, O. V., Schramm, V. L., Zheng, W., and Wolberger, C. (2008) Structural Insights into Intermediate Steps in the Sir2 Deacetylation Reaction. *Structure 16*, 1368–1377.
31. Corda, D., and Girolamo, M. D. (2003) Functional Aspects of Protein Mono-ADP-ribosylation. *EMBO J. 22*, 1953–1958.
32. Di Girolamo, M., Dani, N., Stilla, A., and Corda, D. (2005) Physiological Relevance of the Endogenous Mono(ADP-ribosyl)ation of Cellular Proteins. *FEBS J. 272*, 4565–4575.
33. Lin, H. (2007) Nicotinamide Adenine Dinucleotide: Beyond a Redox Coenzyme. *Org. Biomol. Chem. 5*, 2541–2554.
34. Tanny, J. C., Dowd, G. J., Huang, J., Hilz, H., and Moazed, D. (1999) An Enzymatic Activity in the Yeast Sir2 Protein That Is Essential for Gene Silencing. *Cell 99*, 735–745.
35. Liszt, G., Ford, E., Kurtev, M., and Guarente, L. (2005) Mouse Sir2 Homolog SIRT6 Is a Nuclear ADP-ribosyltransferase. *J. Biol. Chem. 280*, 21313–21320.
36. Haigis, M. C., Mostoslavsky, R., Haigis, K. M., Fahie, K., Christodoulou, D. C., Murphy, A. J., Valenzuela, D. M., Yancopoulos, G. D., Karow, M., Blander, G., Wolberger, C., Prolla, T. A., Weindruch, R., Alt, F. W., and Guarente, L. (2006) SIRT4 Inhibits Glutamate Dehydrogenase and Opposes the Effects of Calorie Restriction in Pancreatic [beta] Cells. *Cell 126*, 941–954.

37. Herrero-Yraola, A., Bakhit, S. M. A., Franke, P., Weise, C., Schweiger, M., Jorcke, D., and Ziegler, M. (2001) Regulation of Glutamate Dehydrogenase by Reversible ADP-ribosylation in Mitochondria. *EMBO J. 20*, 2404–2412.
38. Collier, R. J. (2001) Understanding the Mode of Action of Diphtheria Toxin: A Perspective on Progress during the 20th Century. *Toxicon 39*, 1793–1803.
39. Walsh, C. T. (2005) *Posttranslational Modification of Proteins: Expanding Nature's Inventory*, Roberts and Co., Englewood, CO.
40. Abood, M. E., Hurley, J. B., Pappone, M. C., Bourne, H. R., and Stryer, L. (1982) Functional Homology between Signal-Coupling Proteins. Cholera Toxin Inactivates the GTPase Activity of Transducin. *J. Biol. Chem. 257*, 10540–10543.
41. Van Dop, C., Tsubokawa, M., Bourne, H. R., and Ramachandran, J. (1984) Amino Acid Sequence of Retinal Transducin at the Site ADP-ribosylated by Cholera Toxin. *J. Biol. Chem. 259*, 696–698.
42. D'Amours, D., Desnoyers, S., D'Silva, I., and Poirier, G. G. (1999) Poly(ADP-ribosyl)ation Reactions in the Regulation of Nuclear Functions. *Biochem. J. 342*, 249–268.
43. Schreiber, V., Dantzer, F., Ame, J.-C., and de Murcia, G. (2006) Poly(ADP-ribose): Novel Functions for an Old Molecule. *Nat. Rev. Mol. Cell Biol. 7*, 517–528.
44. Jiang, H., Congleton, J., Liu, Q., Merchant, P., Malavasi, F., Lee, H. C., Hao, Q., Yen, A., and Lin, H. (2009) Mechanism-Based Small Molecule Probes for Labeling CD38 on Live Cells. *J. Am. Chem. Soc. 131*, 1658–1659.
45. Fields, G. B., and Noble, R. L. (1990) Solid Phase Peptide Synthesis Utilizing 9-Fluorenylmethoxycarbonyl Amino Acids. *Int. J. Pept. Protein Res. 35*, 161–214.
46. Mattheakis, L., Shen, W., and Collier, R. (1992) DPH5, a Methyltransferase Gene Required for Diphthamide Biosynthesis in *Saccharomyces cerevisiae*. *Mol. Cell. Biol. 12*, 4026–4037.
47. Rostovtsev, V. V., Green, L. G., Fokin, V. V., and Sharpless, K. B. (2002) A Stepwise Huisgen Cycloaddition Process: Copper(I)-Catalyzed Regioselective "Ligation" of Azides and Terminal Alkynes. *Angew. Chem., Int. Ed. 41*, 2596–2599.
48. Link, A. J., and Tirrell, D. A. (2003) Cell Surface Labeling of *Escherichia coli* via Copper(I)-Catalyzed [3 + 2] Cycloaddition. *J. Am. Chem. Soc. 125*, 11164–11165.
49. Tornoe, C. W., Christensen, C., and Meldal, M. (2002) Peptidotriazoles on Solid Phase: [1,2,3]-Triazoles by Regiospecific Copper(I)-Catalyzed 1,3-Dipolar Cycloadditions of Terminal Alkynes to Azides. *J. Org. Chem. 67*, 3057–3064.
50. Tornoe, C. W., and Meldal, M. (2001) *Peptidotriazoles: Copper(I)-catalyzed 1,3-dipolar cycloadditions on solid-phase* (Lebl, M., and Houghten, R. A., Eds.) pp 263−264, American Peptide Society and Kluwer Academic, San Diego.
51. Zhang, J., and Snyder, S. H. (1993) Purification of a Nitric Oxide-Stimulated ADP-Ribosylated Protein Using Biotinylated β-Nicotinamide Adenine Dinucleotide. *Biochemistry 32*, 2228–2233.
52. Adam, G. C., Sorensen, E. J., and Cravatt, B. F. (2002) Trifunctional Chemical Probes for the Consolidated Detection and Identification of Enzyme Activities from Complex Proteomes. *Mol. Cell. Proteomics 1*, 828–835.
53. Liu, S., Milne, G. T., Kuremsky, J. G., Fink, G. R., and Leppla, S. H. (2004) Identification of the Proteins Required for Biosynthesis of Diphthamide, the Target of Bacterial ADP-Ribosylating Toxins on Translation Elongation Factor 2. *Mol. Cell. Biol. 24*, 9487–9497.
54. Howard, M., Grimaldi, J. C., Bazan, J. F., Lund, F. E., Santos-Argumedo, L., Parkhouse, R. M. E., Walseth, T. F., and Lee, H. C. (1993) Formation and Hydrolysis of Cyclic ADP-Ribose Catalyzed by Lymphocyte Antigen CD38. *Science 262*, 1056–1059.
55. Fryxell, K. B., Odonoghue, K., Graeff, R. M., Lee, H. C., and Branton, W. D. (1995) Functional Expression of Soluble Forms of Human CD38 in *Escherichia coli* and *Pichia pastoris*. *Protein Expression Purif. 6*, 329–336.
56. Sauve, A. A., Munshi, C., Lee, H. C., and Schramm, V. L. (1998) The Reaction Mechanism for CD38. A Single Intermediate Is Responsible for Cyclization, Hydrolysis, and Base-Exchange Chemistries. *Biochemistry 37*, 13239–13249.
57. Munshi, C., Aarhus, R., Graeff, R., Walseth, T. F., Levitt, D., and Lee, H. C. (2000) Identification of the Enzymatic Active Site of CD38 by Site-Directed Mutagenesis. *J. Biol. Chem. 275*, 21566–21571.
58. Graeff, R., Munshi, C., Aarhus, R., Johns, M., and Lee, H. C. (2001) A Single Residue at the Active Site of CD38 Determines Its NAD Cyclizing and Hydrolyzing Activities. *J. Biol. Chem. 276*, 12169–12173.
59. Liu, Q., Kriksunov, I. A., Graeff, R., Munshi, C., Lee, H. C., and Hao, Q. (2005) Crystal Structure of Human CD38 Extracellular Domain. *Structure 13*, 1331–1339.
60. Lee, H. C. (2006) Structure and Enzymatic Functions of Human CD38. *Mol. Med. 12*, 317–322.
61. Kowieski, T. M., Lee, S., and Denu, J. M. (2008) Acetylation-Dependent ADP-ribosylation by *Trypanosoma brucei* Sir2. *J. Biol. Chem. 283*, 5317–5326.
62. French, J. B., Cen, Y., and Sauve, A. A. (2008) *Plasmodium falciparum* Sir2 Is an NAD^+-Dependent Deacetylase and an Acetyllysine-Dependent and Acetyllysine-Independent NAD^+ Glycohydrolase. *Biochemistry 47*, 10227–10239.
63. Ahuja, N., Schwer, B., Carobbio, S., Waltregny, D., North, B. J., Castronovo, V., Maechler, P., and Verdin, E. (2007) Regulation of Insulin Secretion by SIRT4, a Mitochondrial ADP-ribosyltransferase. *J. Biol. Chem. 282*, 33583–33592.
64. Michishita, E., McCord, R. A., Berber, E., Kioi, M., Padilla-Nash, H., Damian, M., Cheung, P., Kusumoto, R., Kawahara, T. L. A., Barrett, J. C., Chang, H. Y., Bohr, V. A., Ried, T., Gozani, O., and Chua, K. F. (2008) SIRT6 Is a Histone H3 Lysine 9 Deacetylase That Modulates Telomeric Chromatin. *Nature 452*, 492–496.
65. McDonald, L. J., and Moss, J. (1994) Nitric Oxide and NAD-Dependent Protein Modification. *Mol. Cell. Biochem. 138*, 201–206.
66. Just, I., Wollenberg, P., Moss, J., and Aktories, K. (1994) Cysteine-Specific ADP-ribosylation of Actin. *Eur. J. Biochem. 221*, 1047–1054.
67. McDonald, L. J., and Moss, J. (1994) Enzymatic and Nonenzymatic ADP-ribosylation of Cysteine. *Mol. Cell. Biochem. 138*, 221–226.
68. Lee, H., and Iglewski, W. J. (1984) Cellular ADP-ribosyltransferase with the Same Mechanism of Action as *Diphtheria* Toxin and *Pseudomonas* Toxin A. *Proc. Natl. Acad. Sci. U.S.A. 81*, 2703–2707.
69. Fendrick, J. L., and Iglewski, W. J. (1989) Endogenous ADP-Ribosylation of Elongation Factor-2 in Polyoma Virus-Transformed Baby Hamster-Kidney Cells. *Proc. Natl. Acad. Sci. U.S.A. 86*, 554–557.
70. Iglewski, W. J. (1994) Cellular ADP-ribosylation of Elongation-Factor-2. *Mol. Cell. Biochem. 138*, 131–133.
71. Sayhan, O., Ozdemirli, M., Nurten, R., and Bermek, E. (1986) On The Nature of Cellular ADP-ribosyltransferase from Rat-Liver Specific for Elongation Factor-II. *Biochem. Biophys. Res. Commun. 139*, 1210–1214.
72. Grimaldi, J. C., Balasubramanian, S., Kabra, N. H., Shanafelt, A., Bazan, J. F., Zurawski, G., and Howard, M. C. (1995) CD38-Mediated Ribosylation of Proteins. *J. Immunol. 155*, 811–817.

BI802093G